Astronomical Techniques and Instruments, Vol. 1, May 2024, 187–196

Article Open Access

Design and application of an autonomous Master Control System for a multi-layer magnetic and helioseismic telescope

Liyue Tong[1,2,3], Yingzi Sun[1,2], Xiao Yang[1,2], Jiaben Lin[1,2*], Yuanyong Deng[1,2,3], Xianyong Bai[1,2,3], Bingxiang Wang[1,2], Xiaoming Zhu[1,2], Yang Bai[1,2], Yi Shang[1,2,4], Hui Wang[1,2]

[1]*National Astronomical Observatories*, *Chinese Academy of Sciences*, *Beijing* 100101, *China*

[2]*Key Laboratory of Solar Activity and Space Weather*, *National Space Science Center*, *Chinese Academy of Sciences*, *Beijing* 100190, *China*

[3]*School of Astronomy and Space Science*, *University of Chinese Academy of Sciences*, *Beijing* 100049, *China*

[4]*School of Electrical and Electronic Engineering*, *Wuhan Polytechnic University*, *Wuhan* 430023, *China*

*Correspondence: jiabenlin@bao.ac.cn

Received: February 23, 2024; Accepted: March 12, 2024; Published Online: April 18, 2024; https://doi.org/10.61977/ati2024020

Citation: Tong, L. Y., Sun, Y. Z., Yang, X., et al. 2024. Design and application of an autonomous Master Control System for a multi-layer magnetic and helioseismic telescope. *Astronomical Techniques and Instruments*, **1**(3): 187−196. https://doi.org/10.61977/ati2024020.

Abstract: With the growing significance of space weather forecasting, multi-layer magnetic and helioseismic telescopes are emerging as a key area of research. However, owing to the diverse operational processes and sophisticated hardware configurations of these devices, there is an urgent need for efficient autonomous observation capabilities. An autonomous Master Control System (MCS) can ensure efficient performance, data consistency, and stability, and the prototype presented here adopts a microservices architecture, breaking down the hardware into multiple subsystems and converting their functions into individual services. A central decision-making system leads the operations, supported by three auxiliary systems and three device control systems. Through inter-subsystem service calls, it achieves rapid imaging and spectroscopic monitoring. To verify system stability and observation efficiency, the system was tested on the Solar Full-disk Multi-layer Magnetograph. Experimental results verify this system can operate automatically for 4 consecutive months, acquire photospheric vector magnetic and Doppler velocity fields within a 15-minute interval, and measure chromospheric longitudinal magnetic and Doppler velocity fields in under 180 s. This ensures consistent and stable solar monitoring and serves as a practical methodological benchmark for the development of similar devices.

Keywords: Astronomical instrumentation; Telescopes; Solar optical telescopes; Automated telescopes

1. INTRODUCTION

Space weather forecasting is a rapidly growing field of research[1], and multi-layer magnetic and helioseismic telescopes (MMHTs) are an essential area under development. In the late 1980s and early 1990s, the Global Oscillation Network Group (GONG) investigated the internal structure and dynamical mechanisms of the Sun by measuring its longitudinal magnetic fields and Doppler velocity fields, enabling predictions on solar activity cycles and their consequential impacts on Earth's space weather[2]. However, more detailed vector magnetic field measurements can provide clearer insights into the generation and evolution of solar phenomena. To this end, it is one of the critical scientific objectives of the Solar Magnetism and Activity Telescope (SMAT)[3]. The joint observations from the Solar Magnetic Telescope at Xinjiang Wenquan and SMAT offer comprehensive data support. Furthermore, the Synoptic Optical Long-term Investigations of the Sun (SOLIS) solar telescope in the USA employs multi-spectral line spectroscopy to study the solar magnetic field and uses imaging spectroscopy for detailed examination of the solar velocity field[4]. In recent years, research and application of rapid modulation liquid crystal technology in solar observation have enabled high-time-resolution and three-dimensional dynamic monitoring of the Sun[5]. An example is the Solar Full-disk Multi-layer Magnetograph (SFMM), shown in Fig. 1, deployed in the Meridian Project Phase II. The SFMM system ingeniously employs four specific spectral lines (the photospheric line Fe I at 5324.19 Å, chromospheric lines Hβ at 4861.34 Å and Hα at 6562.8 Å, and Ca II at 8542.1Å) to capture monochromatic images, magnetic fields, and Doppler velocity fields of the solar photo-

Fig. 1. The main component of the SFMM.

sphere and chromosphere through dual-terminal devices.

To achieve rapid multi-band imaging and spectroscopic observations of the Sun, MMHTs critically require an autonomous MCS to address complex operational processes and challenges associated with multiple devices. In such intricate scenarios, human operations will give rise to inconsistencies in operational processes, causing discrepancies in data production cycles. Additionally, long working hours lead to operator fatigue, significantly increasing the probability of operator errors occurring. The MCS serves as an integration platform for electric control functions of the telescope and its auxiliary hardware, effectively scheduling and coordinating various observation devices while fully assuming responsibility for automating the execution of the entire observational workflow. It enforces strict adherence to uniform operating procedures and data processing standards. In this application, the MCS ensures efficient and stable operation of the entire observational system, thereby guaranteeing consistent processes and high-quality data.

Given the unique optical, mechanical, and electronic designs of telescopes, tailored to their individual scientific objectives, it is impossible to apply a uniform standard in designing a MCS. Consequently, the MCS for different telescopes requires distinctively customized features. For instance, the core functionality of the Automatic Imaging Telescope (AIT) control system lies in achieving fully automated observation procedures[6]. By contrast, the control system of the Gemini telescope places greater emphasis on assisting operators with efficient control[7]. In the case of the Atacama Submillimeter Telescope Experiment (ASTE), located in a remote area, its control system has been fortified with advanced capabilities for remote operation[8], while the Goode Solar Telescope (GST) at Big Bear Solar Observatory (BBSO) uses a Telescope Control System (TCS) which prioritizes user-friendliness and adaptability[9]. Moreover, these MCSs must also demonstrate compatibility with new equipment, as evidenced by the redesign of the LAMOST telescope to an observational control system able to accommodate scalability needs[10].

Despite the benefits of using general-purpose telescope control software or standards to simplify and expedite MCS development, the specificity inherent in individual telescopes necessitates independent development that is not reliant on common standards, and this remains an essential aspect. Currently, widely adopted universal telescope control software and standards include but are not limited to Instrument Neutral Distributed Interface (INDI) (http://www.indilib.org/), Robotic Telescope System 2 (RTS2) (http://rts2.org/)[11], Astronomy Common Object Model (ASCOM) (http://ascom-standards.org/)[12], Observatory Control and Astronomical Analysis Software (OCAAS)[13], and Automatic Telescope Instruction Set （ATIS)[14], all of which have played significant roles in constructing and applying telescope control systems. However, each of these standards and frameworks has its limitations: ATIS may fall short in terms of universality and user-friendliness; OCAAS, as an older software platform, might struggle to fully accommodate new observation equipment; ASCOM, despite its widespread use, faces challenges in hardware driver updates and standardization scope, and; RTS2 and INDI encounter varying degrees of compatibility issues with hardware drivers. The unique components of MMHTs, which are not adequately supported by existing universal standards, create a scenario where strict adherence to these standards would likely introduce substantial system complexity and potentially fail to satisfy its precise scientific requirements. Consequently, to meet the stringent criteria for high-temporal-spatial-resolution observations, as well as ensure flexible monitoring and consistent operational stability, it is imperative to develop a tailor-made MCS designed specifically for the specifications of a MMHT.

Here, we shall employ the SFMM as a paradigm to explain and illustrate the intricate design and operational implementation of a MCS tailored for MMHTs. Sections 2 and 3 elucidate the hardware composition and observation modes of the SFMM system. Section 4 then delves into the overall design scheme for the MCS, encompassing its design philosophy and system functionalities. Section 5 presents the temporal resolution of the SFMM system, demonstrating the remarkable performance of the system in terms of observational precision. The paper concludes with a summary and an outlook on future work.

2. HARDWARE COMPOSITION OF THE SFMM

In the course of multi-band imaging and spectroscopic observations, numerous hardware devices are intricately coordinated and interdependent, each with distinct functions that also continuously change in status during the observation process. Therefore, to construct a more streamlined and efficient MCS, it is essential to decouple and categorize these hardware components according to their individual functionalities.

Based on the functional division of the SFMM hardware components and their integration in terms of spatial

configuration, the system can be primarily summarized into four critical segments: the telescope, outdoor support structure, equatorial mount apparatus, and the observation control room, as shown in Fig. 2. In this schematic diagram, all components except for the imaging optical elements are within the control scope of the MCS.

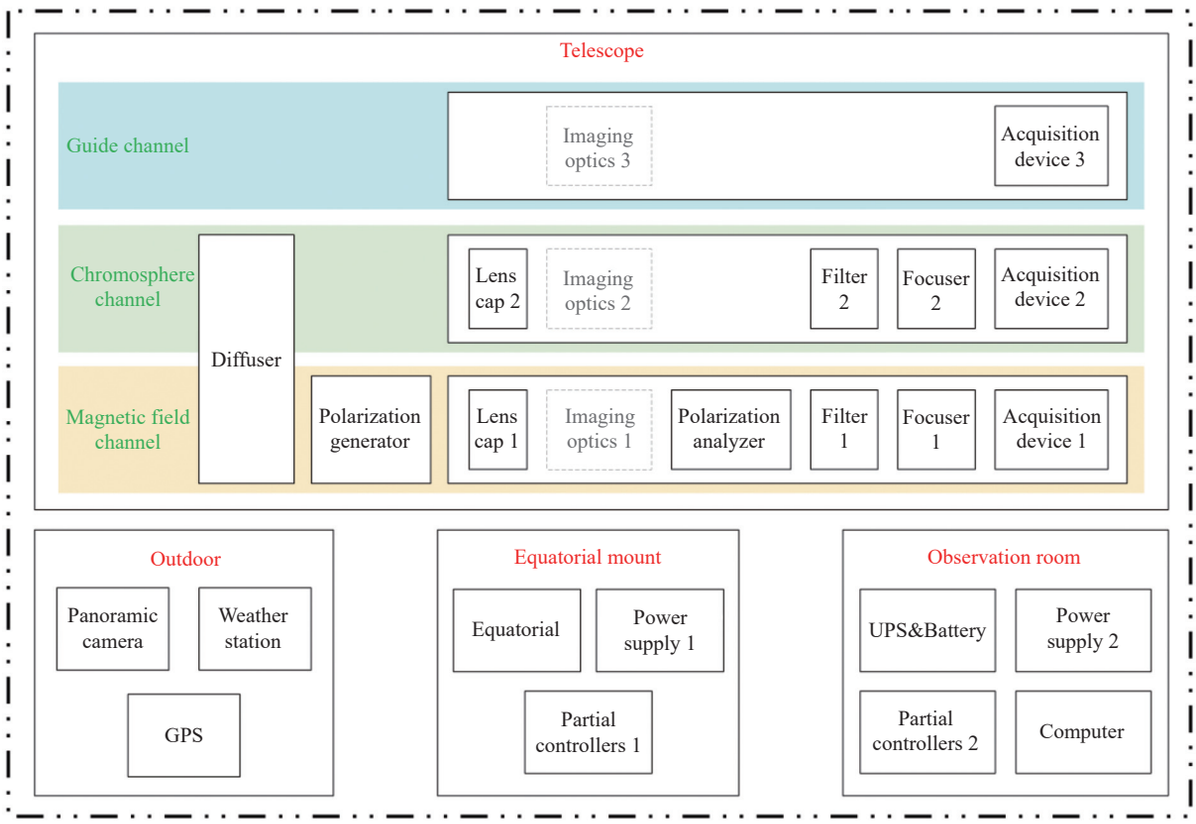

Fig. 2. Hardware composition of the SFMM.

(1) The telescope section is the core of the entire hardware system and is composed of three channels: the magnetic field channel, the chromosphere channel, and the guiding channel. Specifically:

1) The magnetic field channel comprises components such as the lens cap 1, diffuser, polarization generator, imaging optics elements 1, polarization analyzer, filter 1, focuser 1, and acquisition device 1. Its primary function is to acquire monochromatic images at the photospheric line Fe I at 5324.19 Å (abbreviated as 5324), along with corresponding vector magnetic fields and Doppler velocity fields, as well as monochromatic images at the chromospheric line Hβ at 4861.34 Å (abbreviated as 4861), complete with longitudinal magnetic fields and Doppler velocity fields.

2) The chromospheric channel comprises components such as lens cap 2, diffuser, imaging optics elements 2, filter 2, focuser 2, and acquisition device 2. It is dedicated to acquiring monochromatic images of the chromospheric lines Hα at 6562.8 Å (abbreviated as 6563) and Ca II at 8542.1 Å (abbreviated as 8542), measuring their respective Doppler velocity fields.

3) The guiding channel integrates the imaging optics 3 with the acquisition device 3, primarily serving to provide closed-loop control for telescope pointing and tracking, ensuring that the Sun is accurately positioned at the center of the field of view for each channel.

(2) The outdoor section consists of a panoramic camera, a weather station, and a Global Positioning System (GPS). Its primary function is to provide time synchronization, environmental conditions, and full-disk cloud coverage analysis, providing essential environmental decision-making criteria for observations.

(3) The equatorial mount section consists of the equatorial, power supply 1, and partial controllers 1. It serves to guarantee the electrical power supply and mechanical drive for the telescope.

(4) The observation room section primarily consists of Uninterruptible Power Supply (UPS) and Battery, power supply 2, partial controllers 2, and a computer. Its role is to provide the hardware foundation for overall power supply monitoring, residual control, and the scheduling of observational tasks.

3. OBSERVATION MODE OF THE SFMM

Hardware state changes constitute the foundation of

control and scheduling in the MCS. Therefore, analyzing the observation modes of the SFMM is a prerequisite for the implementation of the total control system. According to the observational objectives, the observations made by the SFMM can be categorized into scientific observations and calibration observations. Scientific observations refer to imaging, magnetic field measurements, and Doppler velocity field observations conducted through the magnetic field channel, as well as imaging and Doppler velocity field observations carried out through the chromospheric channel. Calibration observations, on the other hand, include focal length adjustment, flat and dark field calibration, wavelength calibration for both the magnetic field and chromospheric channels, and polarization calibration specifically for the magnetic field channel.

3.1. Scientific Observation Mode

Scientific observations, which represent the primary observation mode following system startup, include acquiring monochromatic images across different wavebands, as well as measuring magnetic fields and Doppler velocity fields.

Presently, the solar magnetic field is mainly measured based on the Zeeman effect. The SFMM will carry out measurements at several wavelength positions around a Zeeman-sensitive photospheric spectral line using narrowband filters and analyze the Stokes polarization parameters (I, Q, U, and V) of the incident light at each spectral position using the polarization modulator. With these observations, we can derive the vector magnetic field. Consequently, magnetic field measurement by a solar telescope is essentially a polarization measurement, i.e., the measurement of Stokes parameters I, Q, U, and V.

Polarization measurements with the SFMM use a differential method. Taking the Q parameter as an example, the detected intensities P (I + Q) and P (I – Q) are obtained through polarization modulation, and the difference between P (I + Q) and P (I – Q) is used to obtain the Q parameter. The sum of these is I. To improve the signal-to-noise ratio, short exposure, alternating sampling, and integration for P (I + Q) and P (I – Q) are applied[15].

After measuring intensity at multiple wavelength positions near the center of the working spectral line, the offset from the line center is calculated by fitting the spectral contour at multiple wavelength points. The solar line-of-sight Doppler velocity can be obtained according to the proportional relationship between Doppler velocity and the drift of the line center[3]. Here, this process is referred to as WaveScan (see, for example, the chromospheric channel's 6 563/8 542 WaveScan in Fig. 3).

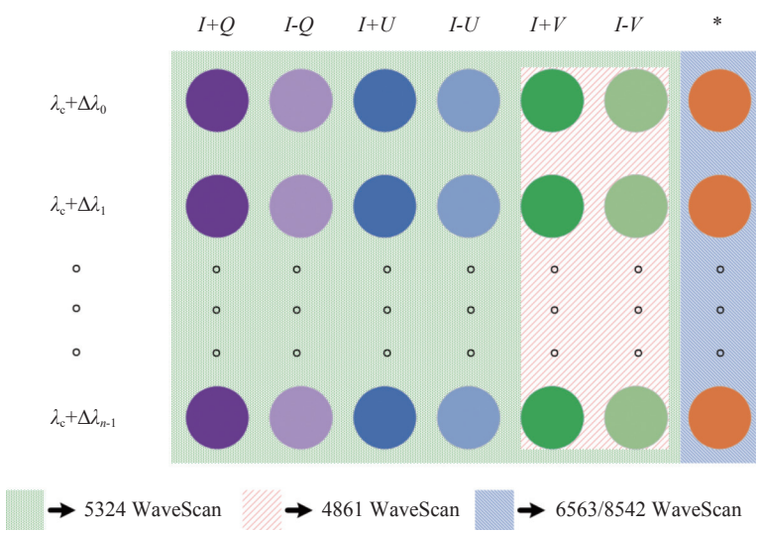

Fig. 3. The overview of data in the magnetic field and Doppler velocity field.

To improve observational efficiency, the SFMM integrates these measurements into a joint observation, as exemplified by the 5324/4861 Wavescan shown in Fig. 3. Additionally, for obtaining higher-resolution chromospheric magnetic field data, this channel implements deeper integration when measuring magnetic fields at the wings of the 4861 line, which is shown in the 4861 LineWing section of Fig. 4.

In the chromospheric channel, imaging observations with higher temporal resolution at the 6563 and 8542 bands of the chromosphere are of particular interest. Therefore, the SFMM has set up high-time-resolution imaging observations at the line center for both the 6563 and 8542 bands (as shown in Fig. 4, at the 6563/8542 LineCenter).

Generally, the observations of both magnetic field channels and chromospheric channels follow a continuous loop pattern, as illustrated in Fig. 4, where:

(1) For magnetic field channels: The cycle typically runs through 5324 WaveScan to 4861 WaveScan, and then onto 4861 LineWing. Upon completion of the observation at the 4861 LineWing, the process restarts from the 5324 WaveScan, continuing iteratively.

(2) For chromospheric channels: The sequence progresses from 6563 WaveScan to 6563 LineCenter, then

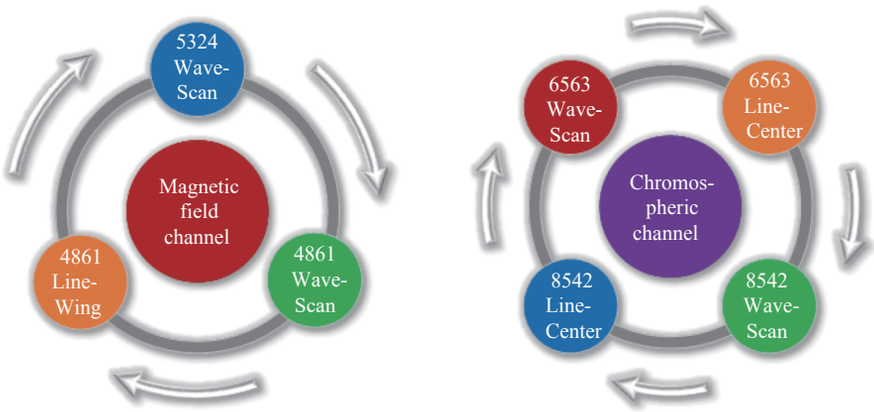

Fig. 4. Mission cycle of scientific observation mode.

moves to 8542 WaveScan, and culminates at 8542 LineCenter. Following the end of the observation at the 8542 LineCenter, it begins again with the 6563 WaveScan, repeating cyclically.

3.2. Calibration Observation Mode

Calibration observations are performed for the calculation of certain inherent properties of the telescope itself to ensure the consistent quality of scientific data. The main aspects include adjustments to the imaging focal length, compensating for any non-uniformities in imaging, calibration of the wavelength accuracy of filters, and polarization calibration of the telescope.

(1) Focal length calibration is performed to guarantee that the SFMM maintains its optimal focus throughout long-term observations. Since daily variations are relatively minor, this calibration is conducted once per quarter, and it has been automated with an autofocus system.

(2) Flat and dark field calibrations serve to eliminate the telescope's influence on imaging results. Under suitable observing conditions, these measurements are executed once daily.

(3) The process of wavelength calibration serves to quantify and correct wavelength drifts induced by variables such as temperature fluctuations and the intrinsic optical system biases within a telescope, thereby ensuring the precise wavelength performance of the filter. This is crucial for accurately measuring Doppler velocity fields. In the SFMM, the relative change in wavelength is derived from the flat and dark field calibration observation process, while the absolute wavelength calibration further accounts for factors such as the Earth's rotational velocity relative to the Sun and annual variations (which generally have a smaller impact).

(4) Polarization calibration compensates for the instrumental polarization of the telescope. The inherent daily variations in the telescope's instrumental polarization are relatively minor, so polarization calibration is usually carried out on a monthly or quarterly basis.

In the calibration process of the SFMM, flat and dark field calibrations are conducted most frequently. Consequently, we have designed and optimized their specific procedures to enhance efficiency. Given that both the magnetic field channel and the chromospheric channel share a single diffuser, the system adopts an interleaved execution strategy. Initially, it performs flat field calibration for the magnetic field channel while conducting dark frame measurements for the chromospheric channel. After both channels complete their current measurements, the magnetic field channel proceeds to its dark frame calibration, and the chromospheric channel carries out its flat field calibration, as illustrated in Fig. 5.

4. AUTONOMOUS IMPLEMENTATION OF THE MCS ON THE SFMM

Based on the above analysis, we have identified that the SFMM is a highly complex and tightly coupled system. To create a loosely coupled and highly cohesive autonomous control system, we have developed the MCS using a microservices architecture[16]. According to the observation modes of the system and considering the inherent properties of individual components, we group components with similar functionalities into a single module and then abstract these related components as one or several services. These services are encapsulated into separate subsystems, as shown in Fig. 6.

In this context, TCS stands for Telescope Control System, which primarily handles the pointing and tracking functions of the telescope; ICS refers to the Instrument Control System, mainly responsible for controlling other components that affect imaging aside from terminal imaging devices; and OCS is the Observation Control System, primarily tasked with executing control functions related to data acquisition during observations. Collectively, the TCS, ICS, and OCS form the core control layer of the MCS.

CCS is the Communication Control System, employing lightweight communication methods to ensure stable communication among all subsystems; PMS is the Power Management System, primarily in charge of managing power supply and backup for the entire system, and EPS, the Environmental Perception System, is designed to sense the environment around the telescope. The CCS,

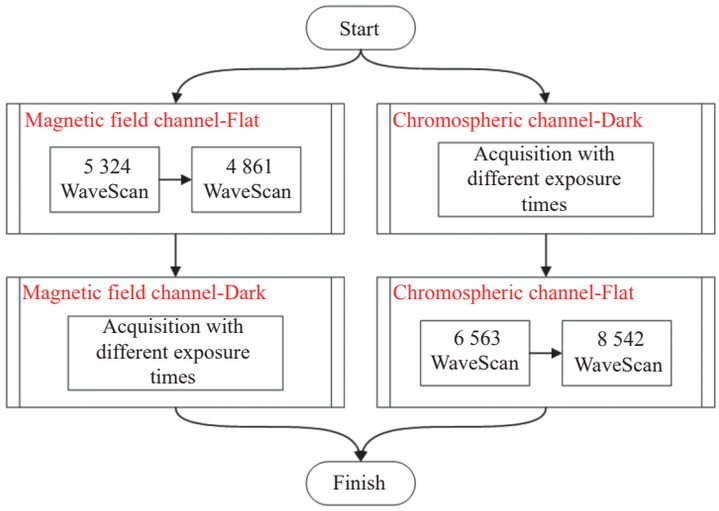

Fig. 5. The flat field and dark frame calibration observation process.

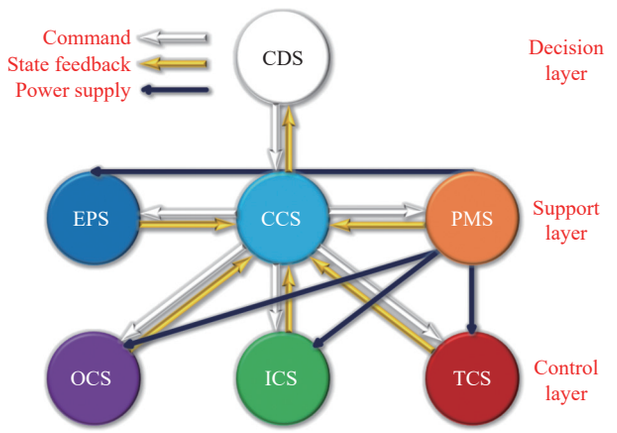

Fig. 6. Compositions of the MCS.

PMS, and EPS together comprise the auxiliary support layer of the total control system.

The Central Decision System (CDS) aggregates services from other systems and, based on the current system status, implements appropriate observation strategies, functioning as the highest decision-making tier of the MCS.

Finally, to minimize system complexity, each subsystem has its own independent user interface, allowing for separate development using different technology stacks. Each subsystem possesses its own state monitoring capabilities, error handling mechanisms, and database, enabling standalone deployment.

4.1. Telescope Control System

High-precision pointing and tracking are essential for the normal operation of a telescope. Therefore, we categorize components, such as the equatorial mount and guiding channel components, into the TCS.

In order to achieve high precision pointing, we have constructed an error model based on spherical harmonics[17], which is used to correct pointing errors. Currently, our pointing accuracy reaches 5″. For closed-loop tracking, the guiding channel calculates the displacement of the solar disk's center of mass and communicates this displacement to the equatorial mount for adjustments[18], thereby achieving a displacement of RMS<1″/30 min for closed-loop tracking errors, as shown in Fig.7.

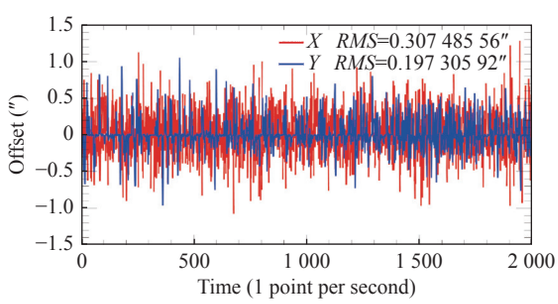

Fig. 7. The closed-loop tracking accuracy of TCS.

4.2. Instrument Control System

After the telescope has stably tracked the Sun, factors affecting imaging within the optical path become critical for achieving scientific objectives. Therefore, components other than the terminal imaging devices that influence imaging are combined into the ICS. When the observer or MCS needs to change the imaging wavelength bands, focal lengths, or polarization states, it can be done solely through controlling ICS.

The ICS is the subsystem in the MCS with the most controlled components and the most frequent scheduling requirements. Its coordination with other subsystems includes functions such as:

(1) Cooperation among the lens cap, diffuser, and acquisition terminal during flat and dark field calibration.

(2) Coordination between the polarization generator, polarization analyzer, and acquisition terminal during polarization calibration.

(3) Coordinating the focuser and acquisition terminal during focal length calibration.

(4) High-speed synchronization of the polarization analyzer with acquisition terminal during magnetic field measurements.

(5) Coordinating the filter and acquisition terminal during velocity field measurements.

The ICS is crucial to the imaging and spectroscopy quality of the entire system. To ensure its stable operation, an additional debugging mode has been set up, allowing observers to view the real-time status of each unit of the system and make necessary adjustments according to their needs.

4.3. Observation Control System

All calibration and scientific data in the system are acquired, stored, and previewed by the acquisition terminal, as described in Section 3.2. This involves multiple acquisition strategies that coordinate with other hardware components, which are difficult to simply classify under any other subsystem. Therefore, we have independently established the OCS for the terminal acquisition component.

To ensure consistent intensity values of solar images during measurements and prevent overexposure or underexposure, we have designed an automatic exposure algorithm. This algorithm adjusts the exposure time based on whether the average intensity of the solar disk falls within a predetermined range, ensuring that the imaging intensity remains approximately constant during observations. This establishes a uniform standard for exposure, providing a foundation for automated data acquisition.

In addressing variations in optical focal length caused by temperature changes and seasonal shifts, we have also devised an automatic focusing algorithm, which acquires multiple short-exposure frames and analyzes their frequency spectrum structure to determine the optimal focal distance at the terminal. It then coordinates this adjustment with the focuser component within the ICS, to enable automatic focusing functionality.

Additionally, when solar flares occur, to provide higher temporal resolution data, we have implemented a flare mode (or rapid mode)[19] in the 6563 and 8542 bands. After the observer activates this mode, the system can record data at a rate of up to one frame per second at a size of 4k × 4k pixels, thereby enabling high-time-resolution observations of solar flare events.

4.4. Communication Control System

After decoupling the system into various subsystems with distinct functionalities and implementing distributed control, stable and reliable communication among these subsystems becomes a critical issue. To facilitate system user management, device management, and overall message management, we have constructed a CCS.

The core functionality of the CCS is to serve as the bridge for communication between different subsystems, facilitating message routing. Hence, to ensure robust system communication, we have developed a lightweight TCP/IP-based communication protocol. This protocol is divided into three parts (shown in Fig. 8): the header (shown in red), the body (green), and the footer (blue). The header contains information describing the message body, facilitating parsing and forwarding tasks; the body carries the specific content of the current message being sent, and the footer provides data verification through a message digest created using the SHA-512 algorithm. Each complete message must not exceed 256×1024 bytes. If a message exceeds this size limit, it will be segmented into several subpackets.

Fig. 8. Communication protocols of CCS.

Apart from the CCS, each subsystem embeds a communication module that incorporates this protocol. When a subsystem starts up or shuts down, it registers or deregisters itself with the CCS, which then updates the online device list and broadcasts it to all subsystems, guaranteeing that the device status list remains available at all times. This arrangement allows decoupling among the subsystems from a communication standpoint, thereby ensuring stable and reliable communication across the entire system.

4.5. Power Management System

During the operation of the telescope, sudden power outages can cause severe damage to components. To prevent such events from occurring, we have designed a PMS, primarily tasked with controlling the indoor and outdoor power supplies for the entire system, as well as monitoring backup power.

In response to issues like power interruptions or voltage fluctuations, we have integrated an UPS at the initial stage of the electrical system. When mains power is normal, the entire system operates in mains-powered mode, with the UPS ensuring a stable supply voltage.

However, when mains power becomes abnormal, the system switches to battery powered mode, with the UPS powering the system. Regardless of the operating mode, the PMS supplies the CDS with information on the current power supply mode, battery health status (State of Health, SOH), current load percentage, and an estimated backup time. These parameters assist the CDS in formulating and evaluating observation strategies.

Additionally, to facilitate easier error handling by the MCS, the power monitoring part of the PMS accurately monitors the power supply to each controlled component.

In case of a failure in any component, PMS can directly disconnect power to that specific component without affecting the normal operation of any other components. After repairs are completed, the PMS will then restore power to that isolated component alone. This achieves decoupling of power supplies among different components, enabling isolated error handling.

4.6. Environmental Perception System

Observations with solar optical telescopes rely heavily on favorable weather conditions and a uniform time standard. Weather variations impact the feasibility of system observations, and a consistent time reference impacts the precision of TCS pointing and the usability of OCS data. Consequently, we have combined a weather station, panoramic camera, and GPS timing system to form an EPS that monitors the weather, analyzes full-disk cloud coverage, and ensures a synchronized system clock, as shown in Fig 9.

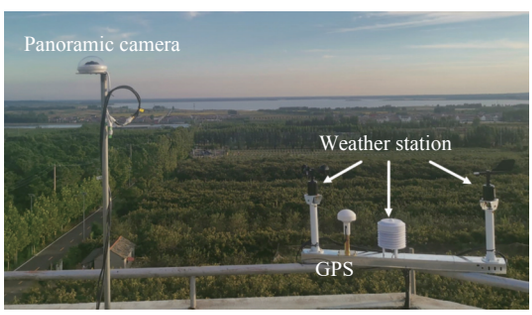

Fig. 9. Hardware foundations of the EPS.

In weather monitoring, temperature readings are crucial for determining thermal management strategies for specific system components, and humidity measurements help assess current rain potential and trigger protection when necessary. The interaction between light intensity sensors and the panoramic camera enables assessment of whether there is any current cloud obstruction. Monitoring PM 2.5 & PM 10 particulate matter concentrations indicates whether foggy or hazy conditions are present. Finally, tracking wind speed and direction allows for decisions about adjusting the TCS tracking strategy.

During solar observations, periods of cloud cover significantly decrease the availability of data. To evaluate the current presence or imminent likelihood of clouds obstructing the view, we employ the panoramic camera to analyze the total cloud coverage throughout the day, providing reliable data on cloud quantities.

4.7. Central Decision System

To further enhance the cohesion of the MCS, we have designed a CDS that unifies services and statuses across all subsystems to facilitate system control and scheduling. The CDS primarily monitors the status of the entire system, controls critical functions, plans and executes observation schedules, autonomously conducts routine observations or follows observation plans pre-set by the observer.

To enable autonomous operation of the total control system in different scenarios such as power outages and cloud obstructions, we have designed different system states for the CDS. These states help the CDS identify the current stage of action execution, facilitating the execution of the next action.

Upon initialization, the CDS is in an unknown state and continuously checks in the background when on standby. In this unknown state, neither observations nor calibrations can be performed, nor can the system be shut down. After an operator or the system initiates startup, the CDS transitions to the booting-up state, then moves to standby once the boot process completes. After executing observation or calibration tasks, the state changes to 'Observing' or 'Calibrating', reverting back to standby upon completion. When an operator or the system initiates shutdown, the CDS enters the shutting-down state and cycles through checking if the shutdown has been completed. If a restart is required, the state switches from 'Shutdown' back to 'Booting-up', as shown in Fig. 10.

When the CDS detects a power anomaly, it cyclically checks whether conditions meet the pre-shutdown state, as depicted in Fig. 10, and if so, it autonomously executes the shutdown procedure. Conversely, when power is restored and there are no cloud obstructions, it cyclically checks whether conditions align with the pre-bootup state. As shown in Fig. 10, when these conditions are met, the

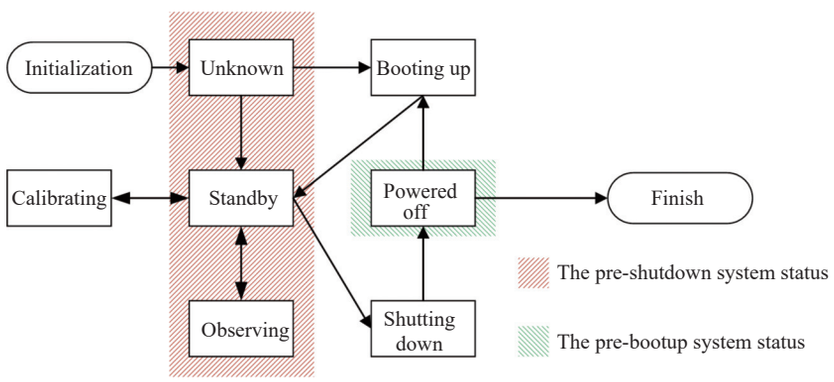

Fig. 10. The state transition diagram of the CDS.

CDS autonomously starts up and resumes observations.

5. STATISTICS ON OBSERVATION EFFICIENCY OF THE SFMM

To validate the observational efficiency of the MCS, we selected observation data from the SFMM on January 23, 2024. We analyzed the time spent on magnetic field and velocity field measurements during each observation cycle as follows:

(1) For vector magnetic field and velocity field measurements in the 5324 Å band, when the exposure time falls within the range of 10 to 20 ms (a value affected by weather and other factors), the detector operates at a frame rate of 8 frames per second. Typically, with an integral frame count of 256 frames and measurements of the velocity field at 6 distinct wavelength positions, the duration for each cycle is less than 15 min (900 s), as shown in Fig. 11.

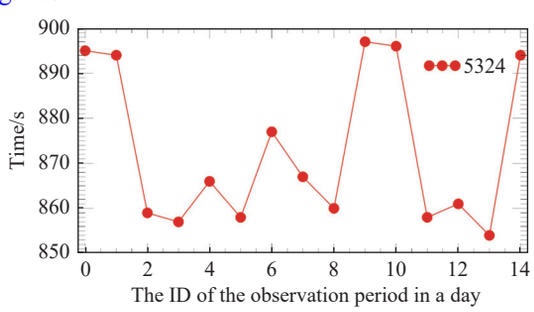

Fig. 11. Temporal Resolution of 5324 WaveScan.

(2) In the case of longitudinal magnetic field and velocity field measurements in the 4861 Å band, when the exposure time falls within the range of 40 to 60 ms (a value affected by weather and other factors), the detector operates at a frame rate of 8 frames per second. Typically, with an integral frame count of 16 frames and measurements of the velocity field at 12 distinct wavelength positions, the time taken for each cycle is less than 180 s, as shown in Fig. 12.

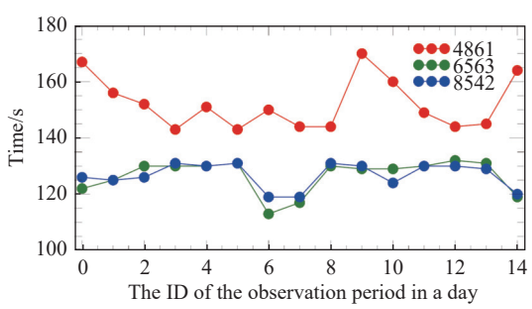

Fig. 12. Temporal resolution of 4861, 6563, 8542 WaveScan.

(3) For velocity field measurements in the 6563/8542 Å bands, when the exposure time falls within the range of 8 to 15 ms (a value affected by weather and other factors), the detector operates at a frame rate of 4 frames per second. Typically, with an integral frame count of 16 frames and measurements of the velocity field at 11 distinct wavelength positions, the duration for each cycle is less than 150 s, as shown in Fig. 12.

From these results, it can be concluded that in the autonomous observations by the MCS of the SFMM, the time cadence for vector magnetic field and velocity field measurements in the photospheric Fe I line at 5324.19 Å is less than 15 minutes. Moreover, the time cadence for longitudinal magnetic field and velocity field measurements in the chromospheric Hβ line at 4861.34 Å, as well as velocity field measurements in the chromospheric Hα line at 6562.8 Å and Ca II line at 8542.1 Å, are all less than 180 s. These results showcase the consistent performance of the autonomous MCS in reliably scheduling device operations and maintaining stability throughout the observation periods for a MMHT, thereby demonstrating its effectiveness in ensuring a steady execution according to the intended cycle, as well as its robustness in terms of system stability during continuous observations.

6. CONCLUSION

The deployment of a MMHT in future solar activity monitoring is becoming increasingly important, but owing to the complex nature of the hardware of a MMHT and its operational processes, the development of an autonomous MCS presents itself as a pressing issue to be tackled. To this end, we have designed an autonomous MCS and applied it to the SFMM.

We analyzed the controlled component information and observation modes of the SFMM. Subsequently, we grouped components with similar functionalities into individual subsystems: TCS, responsible for telescope pointing and tracking with automatic pointing accuracy reaching 5″, with errors of *RMS*< 1″/30 min for closed-loop tracking; ICS, handling focal plane controls excluding terminal instruments, with coordinated completion of automatic flat and dark field calibration and focal length calibration, regulation of liquid crystal filter bandpass adjustment and constant temperature monitoring, and control of polarization modulation; OCS, managing data acquisition including automatic exposure gain adjustment, automatic flat and dark field calibration and focal length calibration in calibration mode, as well as various automatic acquisitions in scientific mode; CCS, serving as a communication bridge among all subsystems; PMS, monitoring power supply backup; and EPS, detecting environmental conditions around the telescope. By abstracting the functions of these subsystems into a series of services, the CDS can access them and make observational judgments based on the status of each subsystem, invoking their respective services to enable automatic and remote observations. This results in high-resolution imaging and spectroscopy, achieving a time cadence of less than 15 min for the vector magnetic field and Doppler velocity field, shown by photospheric Fe I at 5324.19 Å, and under 180 s for the longitudinal magnetic field and Doppler veloc-

ity field shown by chromospheric Hβ at 4861.34 Å, as well as for the velocity field shown by chromospheric Hα at 6562.8 Å and Ca II at 8542.1 Å.

Additionally, in the manually activated flare mode, the system can capture images using Hα at 6562.8 Å or Ca II at 8542.1 Å at a rate of up to one frame per second in 4k × 4k, enabling high-time-resolution monitoring of solar flares.

Currently, the PMS provides the CDS with real-time power supply and backup status, allowing the CDS to conduct autonomous observations based on power availability. While the EPS supplies real-time information about cloud coverage, it cannot effectively predict cloud obscuration during the next observation cycle. Thus, the prediction of cloud paths by EPS is a prerequisite for more autonomous observations in the next phase and will be considered in the future.

ACKNOWLEDGEMENTS

We thank the teachers at the Huairou Solar Observing Station for their help. This study is supported by the National Key R&D Program of China (2022YFF0503800), the Chinese Meridian Project, the National Natural Science Foundation of China (11427901), the Strategic Priority Research Program of the Chinese Academy of Sciences (XDA15320102), and the Youth Innovation Promotion Association (2022057).

AUTHOR CONTRIBUTIONS

Liyue Tong created and implemented the MCS concept, performed experiments, analyzed data, and wrote the original draft of the manuscript. Yingzi Sun provided the overall design for the SFMM. Xiao Yang provided visualization of the SFMM observation mode and corrected the language. Jiaben Lin provided critical feedback on the study design. Yuanyong Deng proposed the overall idea. Xianyong Bai provided the observation mode for the SFMM. BingXiang Wang, XiaoMing Zhu, Yang Bai, Yi Shang and Hui Wang contributed to the study design. All authors read and approved the final manuscript.

DECLARATION OF INTERESTS

Jiaben Lin and Xianyong Bai are editorial board members for Astronomical Techniques and Instruments and were not involved in the editorial review or the decision to publish this article. The authors declare no competing interests.

REFERENCES

[1] Lanzerotti, L. J. 2001. Space weather effects on technologies. *Geophysical Monograph Series*, **125**: 11−22.

[2] Harvey, J. W., Hill, F., Kennedy, J. R., et al. 1988. The Global Oscillation Network Group (GONG). *Advances in Space Research*, **8**(11): 117−120.

[3] Zhang, H. Q., Wang, D. G., Deng, Y. Y., et al. 2007. Solar magnetism and the activity telescope at HSOS. *Chinese Journal of Astronomy and Astrophysics*, **7**(2): 281−288.

[4] Balasubramaniam, K. S., Pevtsov, A. 2011. Ground-based synoptic instrumentation for solar observations. In Society of Photo-Optical Instrumentation Engineers (SPIE) Conference Series.

[5] Hou, J. F., Deng, Y. Y., Wang, D. G., et al. 2021. Application and prospect of liquid crystal modulation technology in solar magnetic field detection. *Spacecraft Environment Engineering*, **38**(3): 296−304. (in Chinese)

[6] Tosti, G., Pascolini, S., Fiorucci, M. 1996. The Perugia University Automatic Observatory. *Publications of Astronomical Society of the Pacific*, **108**: 706

[7] Gillies, K., Walker, S. 1996. The Design of the Gemini Observatory Control System. In Proceedings of Astronomical Society of the Pacific Conference Series.

[8] Kamazaki, T., Ezawa, H., Tatematsu, K., et al. 2005. The remote control system for the ASTE Telescope. In Proceedings of Astronomical Society of the Pacific Conference Series.

[9] Yang, G., Varsik, J. R., Shumko, S., et al. 2006. The telescope control system of the New Solar Telescope at Big Bear Solar Observatory. In Society of Photo-Optical Instrumentation Engineers (SPIE) Conference Series.

[10] Tian, Y., Wang, Z., Li, J., et al. 2018. LAMOST CCD camera-control system based on RTS2. *Research in Astronomy and Astrophysics*, **18**(5): 054

[11] Kubánek, P., Jelínek, M., French, J., et al. 2008. The RTS2 protocol. In Society of Photo-Optical Instrumentation Engineers (SPIE) Conference Series.

[12] George, D. B., Denny, R. 2001. ASCOM-progress in technology and applications. In IAPPP Western Wing (USA) 20th Annual Astronomical Photometry and CCD Imaging Symposium.

[13] Downey, E. C., Mutel, R. L. 1996. The University of Iowa automated telescope facility. In Astronomical Society of the Pacific Conference Series.

[14] Davis Philip, A. G., Hayes, D. S. 1988. New directions in spectrophotometry. Worcester: Davis Press.

[15] Ai, G. X., Hu, Y. F. 1986. On principle of solar magnetic field telescope. *Acta Astronomica Sinica*, **26**(2): 173−180.

[16] Newman, S. 2015. Building Microservices: Designing Fine-Grained Systems. 1st ed. Sebastopol: O'Reilly Media.

[17] Morse, P. M., Feshbach, H. 1953. Methods of theoretical physics, New York: McGraw-Hill.

[18] Guo, J. J., Yang, Y. F., Feng, S., et al. 2016. High precision guide method for the solar telescope. *Chinese Science Bulletin*, **61**(10): 1112−1120.

[19] Lin, J. B., Shen, Y. B., Zhu, X. M., et al. 2013. Design of the an automatic observation system for Full-Disk Solar Magnetograms in the HSOS. *Astronomical Research and Technology*, **10**(4): 392−396. (in Chinese)